International Journal of Heat and Mass Transfer 90 (2015) 1232–1240

Contents lists available at ScienceDirect

International Journal of Heat and Mass Transfer

journal homepage: www.elsevier.com/locate/ijhmt

An iterative, analytical method for solving conjugate heat transfer problems

Krishna Shah, Ankur Jain *

Mechanical and Aerospace Engineering Department, University of Texas at Arlington, USA

ARTICLE INFO

Article history:
Received 16 April 2015
Received in revised form 11 July 2015
Accepted 11 July 2015

Keywords:
Conjugate heat transfer
Thermal conduction
Convection
Analytical methods

ABSTRACT

Conjugate heat transfer involving convection and conduction in a fluid flow and a solid body in contact with each other occurs commonly in engineering applications. While analytical solutions for individual convection and conduction problems are relatively easier, it is a lot more challenging to solve the combined conjugate heat transfer problem. In this paper, an iterative method is developed for analytically solving conjugate heat transfer problems. Based on an initial assumption of the temperature field at the solid–fluid interface, the temperature distributions in the fluid and solid body are determined by separately solving the governing energy conservation equations in the two domains. These solutions are used to improve the initial assumption of the interface temperature until convergence. It is found that only a few iterations of this process are needed for convergence. Temperature fields computed from this analytical approach are found to be in good agreement with finite element simulation results. The iterative analytical approach is used to solve two technologically relevant problems related to internal and external flows. Given the general nature of the iterative approach, results from this paper may be helpful in solving a variety of conjugate heat transfer problems.

1. Introduction

Conjugate heat transfer involving coupled conduction and convection is of significance in many engineering systems. A large volume of past research [1–14] has been devoted to solving temperature fields for a fluid flowing in contact with a solid body, wherein thermal convection within the fluid domain occurs in conjunction with conduction within the solid domain. While the effect of conduction in the solid body is important in the thermally developing fluid region [2,15], it is also clearly important in case of internal heat generation in the solid that is being convected by the flowing fluid [16]. This makes it critical to develop analytical solutions for conjugate problems involving convection in fluid flow and conduction in a solid which is in contact with the fluid flow. Problems involving external flow and internal flow are both of interest.

Derivation of solutions for convection-only or conduction-only problems is relatively straightforward. Well-known solutions exist for specific boundary conditions such as constant temperature or constant heat flux [1,4,5]. Similarly, theoretical solutions for a variety of conductions problems are also available [17,18]. However, analytical derivation of temperature distribution in conjugate problems is in general a lot more challenging [19]. A fundamental problem underlying several conjugate heat transfer problems was first solved by Graetz [3,4] who derived an analytical expression for temperature in a fluid flowing through a duct with constant temperature boundary condition, assuming that the flow is hydrodynamically developed and thermally developing. Analytical expressions for eigenvalues and eigenfunctions for this solution have been computed [7], and this solution has been used to derive the solution for a more general problem with continuously or discretely varying wall temperature using linear superimposition [2,7,8]. Boundary layer solution for fluid flow over a plate for thermal boundary layer nonsimilarity arising from both velocity field and streamwise variation of temperature have been analyzed [6]. The case of constant or axially varying wall heat flux has also been analyzed. While axial conduction in the fluid is mostly neglected, some papers have accounted for this phenomenon [9,20], which is relevant for specific technological applications.

While the classical convection problems for internal and external flows do not consider thermal conduction within the solid body in contact with the fluid flow, solutions to these problems provide the basic building block for deriving temperature distributions in conjugate problems where thermal conduction in the solid and thermal convection in the fluid must be considered

* Corresponding author at: 500 W First St, Rm 211, Arlington, TX 76019, USA. Tel.: +1 (817) 272 9338; fax: +1 (817) 272 2952.
E-mail address: jaina@uta.edu (A. Jain).

http://dx.doi.org/10.1016/j.ijheatmasstransfer.2015.07.056
0017-9310/

Nomenclature

α	thermal diffusivity
h	convective heat transfer coefficient
H	height/thickness
k	thermal conductivity
L	length of the plate
Pr	Prandtl number
q	heat flux
Q	volumetric heat generation rate
R	radius
Re	Reynolds number
T	temperature
u	velocity

Subscripts

0	initial value
e	entry
f	fluid
i	inner
o	outer
s	solid
r	radial coordinate
z	axial coordinate
∞	freestream value

Superscript

+	non-dimensional variable

simultaneously. A number of approaches have been presented for solving this conjugate problem. A series form of the wall temperature has been assumed, and energy conservation at the solid–fluid interface has been used to derive expressions for coefficients of the series form [10,11,21], resulting in analytical expressions for the entire temperature distribution. In particular, expressions for pipe flow [10], a plate in liquid or gas flow [11,12], flow between parallel plates [22,23] and for turbulent flows [20] have been presented. A solution for the conjugate problem of flow over a flat plate has also been presented using the method of the asymptotic solution of singular integral equations [13]. In addition to such approaches, the integral transform technique has also been used for solving conjugated heat transfer problems [24,25]. Semi-analytical [26–30] and purely numerical [31–33] techniques have also been used. These papers utilize discretization based on finite-element or finite-difference based methods.

This paper presents a solution for the conjugate heat transfer problem using an iterative approach that utilizes analytical solutions of both conduction and convection problems solved independently. Solutions to these two sub-problems are coupled with each other through temperature continuity and energy conservation at the solid–fluid interface. Both internal and external flow problems are addressed. In this method, the temperature at the solid–fluid interface is assumed, based on which the temperature distribution in the fluid is determined analytically. Using energy conservation at the interface, the solid temperature distribution is then determined. The interface temperature determined from here is used iteratively to improve the wall temperature distribution until reasonable convergence. Such an approach has been used in the past for analytical determination of temperature distribution in thermal conduction problems in a multi-layer solid body [34–36]. In addition, a few papers have also utilized a similar iterative method for semi-analytical solution of conjugate heat transfer problems, wherein a finite-element or finite-difference discretization approach is used to numerically solve the thermal conduction problem [26,28–30]. The present approach which determines both fluid and solid temperature distributions analytically, results in reduced mathematical complexity compared to classical, non-iterative approaches [10–12,20,24], without the need to resort to discretization and numerical techniques used in past semi-analytical approaches [26–30]. It is found that only a small number of iterations are sufficient for reasonable convergence of results. The iterative method is utilized to model conjugate heat transfer in two specific problems – the cooling of a hollow heat generating cylinder with anisotropic thermal conductivity, and the cooling of a heat generating solid block due to fluid flow over the block. These models represent technologically important energy conversion processes, for example, the liquid cooling of an annular Li-ion cell [16] during a high-rate discharge process [37]. The next section presents the general iterative approach, followed by derivation of specific solutions for internal and external flow problems.

2. General solution: the iterative approach

This section presents the general approach for analytically solving a conjugate problem involving thermal conduction and convection in a solid and fluid flow respectively. Consider a solid (**S**) with an arbitrary shape as shown in Fig. 1. Fluid flow **(F)** occurs with a given velocity profile. The solid and fluid intersect at an interface, denoted by **S-F**. In general, internal heat generation within the solid is considered. Although Fig. 1 shows an external flow scenario, in general, fluid flow may occur either over the solid (external flow), or through the solid (internal flow).

In general, the interest is in deriving expressions for temperature distributions $T_s(\bar{x})$ and $T_f(\bar{x})$ where $\bar{x}$ is the general spatial

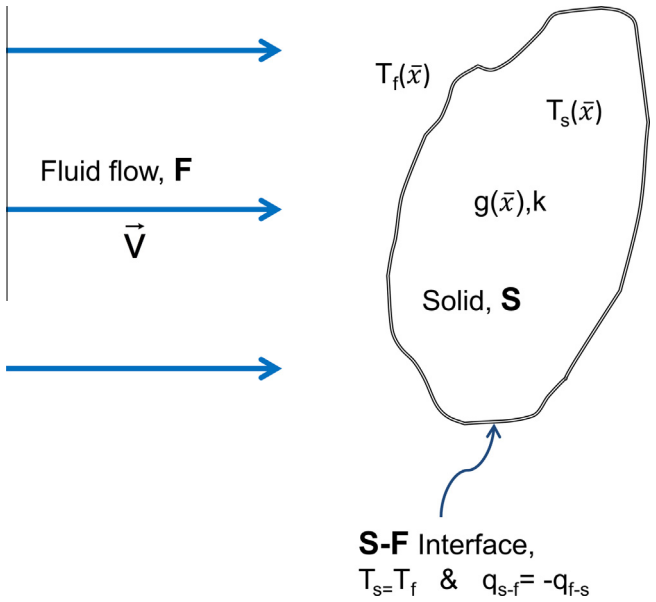

Fig. 1. Schematic of a general conjugate heat transfer problem involving a fluid flow over an arbitrarily shaped solid with internal heat generation.

coordinate. Only the laminar, steady state problem is considered here. The governing conservation equations that must be solved to determine these temperature distributions are given by

$$\alpha\nabla^2 T_f = (\vec{v}\cdot\nabla)T_f + \mu\cdot\Phi + \bar{g}_f \tag{1}$$

and

$$k\nabla^2 T_s + g_s(\bar{x}) = 0 \tag{2}$$

Here, $\mu\cdot\Phi$ is the viscous dissipation, and $\bar{g}_f$ and $\bar{g}_s$ are volumetric heat generation rates in the solid and fluid respectively. The methodology discussed in this paper for deriving analytical solutions for the temperature fields in **S** and **F** is based on analytically solving the temperature fields individually in the solid and fluid domains, and utilizing principles of temperature compatibility and conservation of energy at the interface to iterate until a stable solution is obtained. To start with, the fluid temperature distribution at the interface **S-F** is assumed to be

$$T_f(\bar{x}_{S-F}) = T_0(\bar{x}_{S-F}) \tag{3}$$

Assuming the velocity field in the fluid is known in advance, Eq. (1) can now be solved along with the assumed boundary condition at the interface. Once $T_f(\bar{x})$ is known, the heat flux into the solid at the solid–fluid interface can be obtained by differentiating.

$$q_{s,in}(\bar{x}) = k_f\frac{\partial T_f}{\partial\bar{n}} \tag{4}$$

where $\bar{n}$ is the outward normal to the solid surface at the **S-F**.

Eq. (4) represents a boundary condition for the temperature distribution in the solid $T_s(\bar{x})$. The governing equation (2) can now be solved along with Eq. (4). The solution for $T_s(\bar{x})$ provides a means to determine the temperature of the solid at the interface, which can then be used to update the interface temperature distribution that was assumed in Eq. (3). The entire procedure can be repeated to determine the temperature distributions over multiple iterations. Eventually, the temperature distributions may be expected to converge, with negligible change from one iteration to the next.

The analytical framework described above is used for analyzing both internal and external flows, which are discussed in subsequent sub-sections.

2.1. Internal flow

Consider the laminar flow of a fluid through an annular cylinder, shown schematically in Fig. 2(a). The fluid flow is assumed to be hydrodynamically fully developed when it enters the cylinder, with a given velocity profile $u(r^+)$ and entry temperature T_e at the entrance, $z^+ = 0$. The solid portion of the cylinder is assumed to generate heat with a volumetric rate of Q. Convective heat transfer with coefficients h_{ro} and h_z are assumed over the outer surface and axial faces of the cylinder respectively.

This general solid–fluid problem is commonly encountered in engineering applications, for example, in flow of a cold fluid through a Li-ion cell that generates heat due to electrochemical energy conversion within the cell [16,37]. The interest in is deriving expressions for cell and coolant temperature fields due to a specific internal heat generation rate and coolant flowrate.

To start with, a temperature distribution is assumed at the wall

$$T_f(z^+, r^+ = 1) = T_{wall}(z^+) = T_0(z^+) \tag{5}$$

Neglecting viscous dissipation, heat transfer in the fluid domain is governed by the following governing conservation equation [1],

$$\frac{\partial^2 T_f^+}{\partial r^{+2}} + \frac{1}{r^+}\frac{\partial T_f^+}{\partial r^+} = (1-r^{+2})\frac{\partial T_f^+}{\partial z^+} \tag{6}$$

The non-dimensional coordinates z^+ and r^+ are given by

$$z^+ = \frac{z/R_i}{\mathrm{Re}\cdot\mathrm{Pr}} \tag{7}$$

$$r^+ = \frac{r}{R_i} \tag{8}$$

and temperature is non-dimensionalized as follows:

$$T_f^+ = \frac{T_f}{QH^2/k_r} \tag{9}$$

The temperature solution based on a given T_f^+ (z^+, $r^+ = 1$) is obtained as follows [1]

$$T_f^+(z^+, r^+) - T_e^+ = \int_0^{x^+}[1-\theta(z^+-\xi^+, r^+)]\frac{dT_{wall}^+(\xi^+)}{d\xi^+}d\xi^+ + \sum_{i=1}^{k}[1-\theta(z^+-\xi_i^+, r^+)]\left(T_{wall}^+(\xi_i^+) - T_e^+\right) \tag{10}$$

The integral in Eq. (10) accounts for continuous variations in wall temperature and summation accounts for discrete step changes. Note that the coolant entry temperature T_e^+ could be lower than zero in case the coolant fluid is precooled prior to entering the annular cylinder. This helps analyze the effect of precooling.

The function θ is given by

$$\theta(z^+, r^+) = \sum_{n=0}^{\infty} C_n R_n(r^+)\exp(-\lambda_n^2 z^+) \tag{11}$$

$$T_{wall}^+ = \frac{T_{wall}}{QH^2/k_r} \tag{12}$$

$$T_e^+ = \frac{T_e}{QH^2/k_r} \tag{13}$$

Here, λ_n are the eigenvalues, R_n are the corresponding eigenfunctions and C_n are constants. Analytical expressions for λ_n, R_n and C_n are given by Sellars et al. [7].

Eq. (10) defines the temperature solution within the fluid, from which the wall heat flux can be obtained:

$$q_{wall}^+(z^+) = K\left.\frac{\partial T_f^+}{\partial r^+}\right|_{r^+=1} = -K\left[\int_0^{z^+}\theta_{r^+}(z^+-\xi^+, r^+=1)\frac{dT_{wall}^+(\xi^+)}{d\xi^+}d\xi^+ + \sum_{i=1}^{k}\theta_{r^+}(z^+-\xi_i^+, r^+=1)(T_{wall}^+(\xi_i^+) - T_e^+)\right] \tag{14}$$

where,

$$\theta_{r^+}(z^+, 1) = -2\sum_{n=0}^{\infty} G_n\exp(-\lambda_n^2 z^+) \tag{15}$$

$$q_{wall}^+ = \frac{q_{wall}}{QH^2/R_i}$$

$$K = \frac{k_f}{k_r}$$

Analytical expression for G_n is also provided by Sellars et al. [7]. Eq. (14) provides an analytical basis for computing the heat flux distribution at the solid–fluid interface, given an assumed temperature distribution at the wall. Once the heat flux is determined, the temperature distribution in the solid domain can be computed. In this case, the governing equation for the temperature distribution in the solid domain is

$$H^{+2}\frac{1}{r^+}\frac{\partial}{\partial r^+}\left(r^+\frac{\partial T_s^+}{\partial r^+}\right) + K_s\frac{\partial^2 T_s^+}{\partial z^{+2}} + 1 = 0 \tag{16}$$

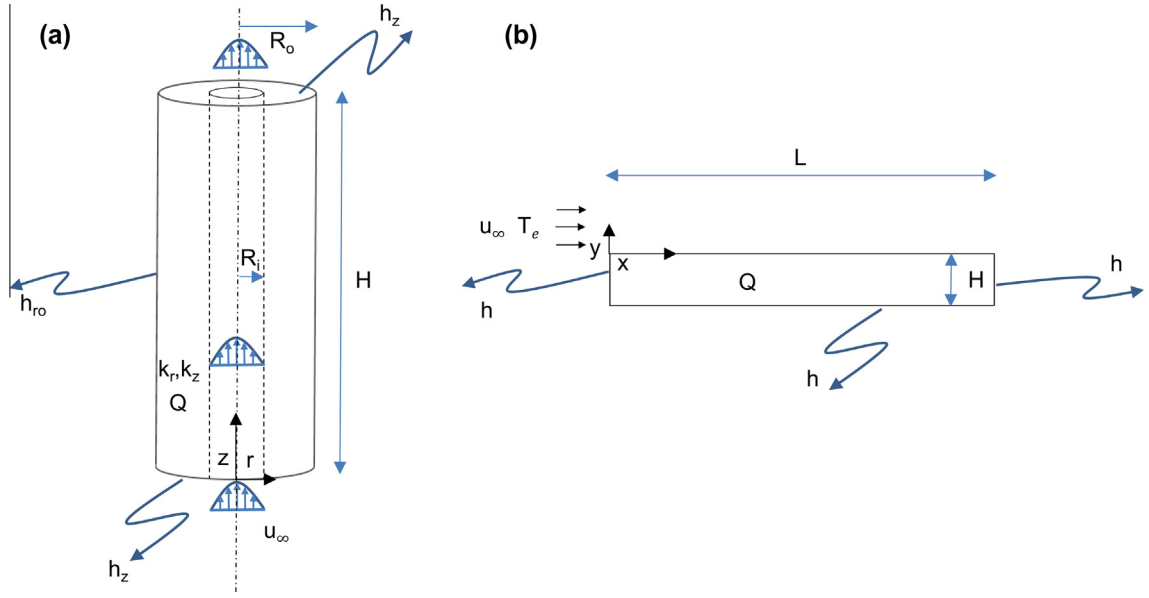

Fig. 2. (a) Schematic of hydrodynamically fully developed flow through an annular cylinder with anisotropic thermal conductivity and volumetric internal heat generation, (b) schematic of fluid flow with constant freestream velocity over a semi-infinite flat plate with volumetric heat generation.

where,

$$T_s^+ = \frac{T_s}{QH^2/k_r} \tag{17}$$

$$z^+ = \frac{z}{H} \tag{18}$$

$$H^+ = \frac{H}{R_i} \tag{19}$$

$$K_s = \frac{k_z}{k_r} \tag{20}$$

Note that thermal conductivities in the radial and axial directions are assumed to be unequal, in order to account for the general case of orthotropic thermal conduction in the Li-ion cell [38].

The governing equation is subject to the following boundary conditions:

$$\frac{\partial T_s^+}{\partial z^+} = Bi_z T_s^+ \quad \text{at } z^+ = 0 \tag{21}$$

$$\frac{\partial T_s^+}{\partial z^+} = -Bi_z T_s^+ \quad \text{at } z^+ = 1 \tag{22}$$

$$\frac{\partial T_s^+}{\partial r^+} = q_{wall}^+(z^+) \quad \text{at } r^+ = 1 \tag{23}$$

$$\frac{\partial T_s^+}{\partial r^+} = -\frac{Bi_{R_o}}{R_o^+} T_s^+ \quad \text{at } r^+ = R_o/R_i \tag{24}$$

where,

$$R_o^+ = \frac{R_o}{R_i} \tag{25}$$

Note that the wall heat flux in the boundary condition at $r^+ = 1$ is obtained based on the solution of the fluid problem. The temperature field may be determined by first splitting $T_s^+(z^+, r^+)$ into two components

$$T_s^+(z^+, r^+) = T_{s1}^+(z^+) + T_{s2}^+(z^+, r^+) \tag{26}$$

$T_{s1}^+(z^+)$ is governed by an ordinary differential equation that includes the heat generation term, whereas $T_{s2}^+(z^+)$ absorbs the non-homogeneity in the boundary condition. These sub-problems can be solved using standard methods [16,17] to derive the following solutions:

$$T_{s1}^+(z^+) = \frac{1}{2K_s}\left[z^+(1-z^+) + Bi_H^{-1}\right] \tag{27}$$

and

$$T_{s2}^+(z^+, r^+) = \sum_{n=1}^{\infty} \left[\left(A_n^+ + B_n^+\right) \cdot I_0(\lambda_n r^+ R_i) + \left(A_n^+ \beta_1 + B_n^+ \beta_2\right) \cdot K_0(\lambda_n r^+ R_i)\right] \cdot \left[\mu_n H Cos(\mu_n H z^+) + Bi_H Sin(\mu_n H z^+)\right] \tag{28}$$

The coefficients A_n^+ and B_n^+ in Eq. (28) are given by

$$A_n^+ = \frac{-\int_0^1 T_{s1}^+(z^+)[(\mu_n H)Cos(\mu_n H \cdot z^+) + Bi_H Sin(\mu_n H \cdot z^+)]dz^+}{\frac{1}{2}[(\mu_n H)^2 + Bi_H^2 + 2Bi_H] \cdot [I_o(\lambda_n R_o) + Bi_{R_o}^{-1}(\lambda_n R_o) \cdot I_1(\lambda_n R_o) + \beta_1(K_o(\lambda_n R_o) - Bi_{R_o}^{-1}(\lambda_n R_o) \cdot K_1(\lambda_n R_o))]} \tag{29}$$

$$B_n^+ = \frac{\int_0^1 q_{wall}^+(z^+)[(\mu_n H)Cos(\mu_n H \cdot z^+) + Bi_H Sin(\mu_n H \cdot z^+)]dz^+}{\frac{1}{2}(\lambda_n R_i)[(\mu_n H)^2 + Bi_H^2 + 2Bi_H] \cdot [I_1(\lambda_n R_i) - \beta_2(K_1(\lambda_n R_i))]} \tag{30}$$

where,

$$\beta_1 = \frac{I_1(\lambda_n R_i)}{K_1(\lambda_n R_i)} \tag{31}$$

$$\beta_2 = \frac{(\lambda_n R_o) I_1(\lambda_n R_o) + Bi_{ro} I_o(\lambda_n R_o)}{(\lambda_n R_o) K_1(\lambda_n R_o) - Bi_{ro} K_o(\lambda_n R_o)} \tag{32}$$

The eigenvalues $\mu_n H$ are obtained from roots of the transcendental equation

$$\mathrm{Tan}(\mu H) = \frac{2Bi_H \cdot (\mu H)}{(\mu H)^2 - Bi_H^2} \tag{33}$$

Further, $Bi_H = \frac{h_z H}{k_z}$, $Bi_{Ro} = \frac{h_{ro} R_o}{k_r}$ and $\lambda_n = \sqrt{\frac{k_z}{k_r}}\mu_n$. Finally, $T_{wall}{}^+(z^+)$ is determined from the solid temperature distribution in Eq. (26) computed at $r^+ = 1$. This provides an update to the initial assumption of $T_{wall}{}^+(z^+)$ shown in Eq. (5) and initiates the next iteration of computing the fluid temperature field, followed by the solid temperature field. In order to avoid divergence, a weighted average of $T_{wall}{}^+$ from the previous iteration and $T_{wall}{}^+$ determined from the solid temperature field may be used for updating $T_{wall}{}^+$ for the next iteration. Iterations are carried out until the change in $T_{wall}{}^+(z^+)$ from one iteration to the next is below a desired threshold.

2.2. External flow

The general approach outlined in Section 2 is now used for solving an external flow problem, in which a fluid with a known freestream velocity flows over a heated solid. The flow is assumed to be laminar. Similar to the problem discussed in Section 2.1, this is also a commonly encountered heat transfer problem. As shown schematically in Fig. 2(b), a semi-infinite flat plate of length L and thickness H generates heat at a volumetric rate of Q. Fluid flow occurs at the top surface with given freestream velocity and temperature of u_∞ and T_e respectively. The plate is also being cooled at the other three surfaces with convective heat transfer coefficient h.

The procedure starts with an assumed temperature distribution $T_{wall}(x)$ on the solid–fluid interface, $y = 0$. Neglecting viscous dissipation, the governing energy equation for the fluid is

$$\frac{\partial^2 T_f^+}{\partial y^{+2}} = u^+\frac{\partial T_f^+}{\partial x^+} + v^+\frac{\partial T_f^+}{\partial y^+} \tag{34}$$

where,

$$T_f^+ = \frac{T_f}{QL^2/k_s} \tag{35}$$

$$x^+ = \frac{x}{L} \tag{36}$$

$$y^+ = \frac{y}{H} \tag{37}$$

$$u^+ = \frac{u \cdot H^2}{\alpha L} \tag{38}$$

$$v^+ = \frac{vH}{\alpha} \tag{39}$$

The solution to Eq. (34) with the assumed wall temperature boundary condition is given by [1]

$$T_f^+(x^+,y^+) - T_e^+ = \int_0^{x^+}\left[1-\theta(\xi^+,x^+,y^+)\right]\frac{dT_{wall}^+}{d\xi^+}d\xi^+ + \sum_{i=1}^{k}\left[1-\theta(\xi_i^+,x^+,y^+)\right]\left(T_{wall}^+(i) - T_e^+\right) \tag{40}$$

where the function $\theta(\xi,x^+,y^+)$ is given by [1]

$$\theta(\xi,x^+,y^+) = \frac{0.331\mathrm{Pr}^{1/3}\mathrm{Re}_x^{1/2}y^+H}{x^+L\left[1-\left(\frac{\xi^+}{x^+}\right)^{3/4}\right]^{1/3}} - \frac{0.005405\mathrm{Pr}\mathrm{Re}_x^{3/2}y^{+3}H^3}{x^{+3}L^3\left[1-\left(\frac{\xi^+}{x^+}\right)^{3/4}\right]} \tag{41}$$

and

$$T_{wall}^+ = \frac{T_{wall}}{QL^2/k_s} \tag{42}$$

$$T_e^+ = \frac{T_e}{QL^2/k_s} \tag{43}$$

The integral and summation terms in Eq. (40) account for the variation in $T_{wall}{}^+$ as a function of x^+, and any step changes that may exist in the $T_{wall}{}^+$ distribution.

Similar to the internal flow problem, the wall heat flux can be computed as follows:

$$q_{wall}^+(x^+) = \frac{q_{wall}(x^+)}{QL^2/H} = -K\frac{\partial T_f^+}{\partial y^+}\bigg|_{y^+=0} = K\left[\int_0^{x^+}\theta_{y^+}(\xi^+,x^+,0)\frac{dT_{wall}^+}{d\xi^+}d\xi^+ + \sum_{i=1}^{k}\theta_{y^+}(\xi_i^+,x^+,0)\left(T_{wall}^+(i) - T_e^+\right)\right] \tag{44}$$

where $K = k_f/k_s$.

By differentiating equation (41) with respect to y^+, $\theta_{y^+}^+(\xi,x^+,0)$ is given by

$$\theta_{y^+}(\xi,x^+,0) = \frac{0.331\mathrm{Pr}^{1/3}\mathrm{Re}_x^{1/2}}{x^+L}\left[1-\left(\frac{\xi^+}{x^+}\right)^{3/4}\right]^{-1/3} \tag{45}$$

$q_{wall}{}^+(x^+)$ computed by Eq. (44) is then used to provide a boundary condition for the energy conservation equation that governs the temperature distribution in solid:

$$\frac{\partial^2 T_s^+}{\partial x^{+2}} + L^{+2}\frac{\partial^2 T_s^+}{\partial y^{+2}} + 1 = 0 \tag{46}$$

where $T_s(x,y)$ is the temperature rise above ambient in the solid.

The governing equation is subject to the following boundary conditions:

$$\frac{\partial T_s^+}{\partial x^+} = Bi_L T_s^+ \quad \text{at } x^+ = 0 \tag{47}$$

$$\frac{\partial T_s^+}{\partial x^+} = -Bi_L T_s^+ \quad \text{at } x^+ = 1 \tag{48}$$

$$\frac{\partial T_s^+}{\partial y^+} = Bi_H T_s^+ \quad \text{at } y^+ = -1 \tag{49}$$

$$\frac{\partial T_s^+}{\partial y^+} = -q_{wall}^+(x^+) \quad \text{at } y^+ = 0 \tag{50}$$

Solution for $T_s{}^+(x^+,y^+)$ proceeds along similar lines as the previous section. The temperature field may be determined by splitting $T_s{}^+(x^+,y^+)$ into two components

$$T_s^+(x^+,y^+) = p^+(x^+) + w^+(x^+,y^+) \tag{51}$$

The two components of the temperature distribution are given by

$$p^+(x^+) = \frac{1}{2}\left[x^+(1-x^+) + \frac{1}{Bi_L}\right] \tag{52}$$

and

$$w(x^+,y^+) = \sum_{n=1}^{\infty}\left[C_n^+ Cosh(\mu_n H y^+) + D_n^+(\beta_n Cosh(\mu_n H y^+) + Sinh(\mu_n H y^+))\right] \cdot \left[\mu_n L Cos(\mu_n L x^+) + Bi_L Sin(\mu_n L x^+)\right] \tag{53}$$

The coefficients $C_n{}^+$, $D_n{}^+$ and β_n in Eq. (53) are given by

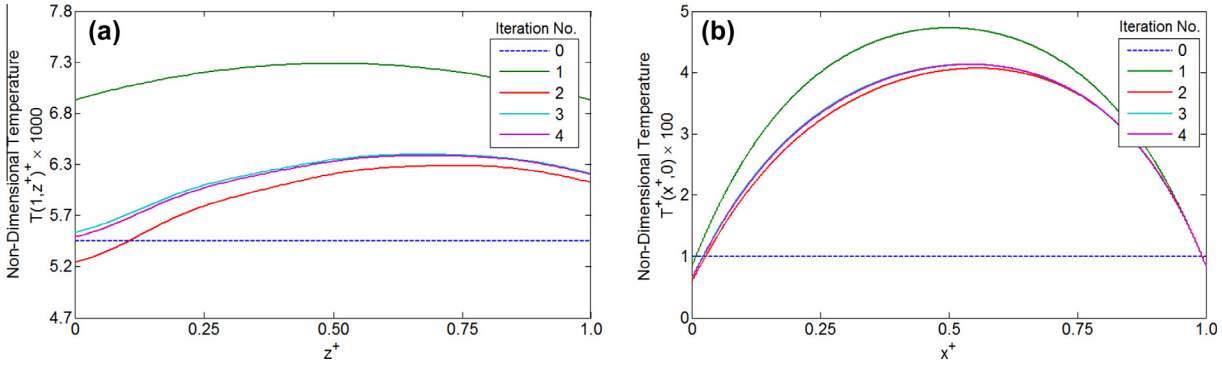

Fig. 3. (a) Temperature distribution along the inner wall as a function of number of iterations for the internal flow problem, (b) temperature distribution along the solid–fluid interface as a function of number of iterations for the external flow problem.

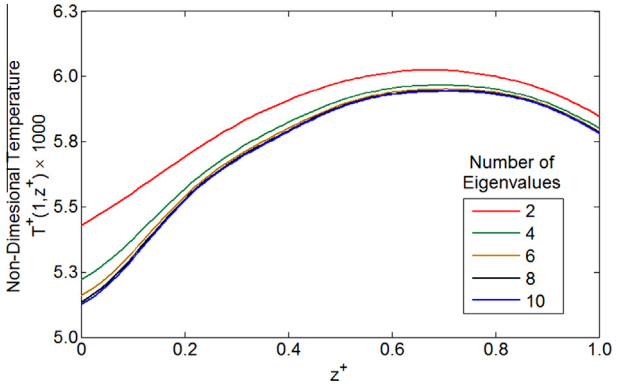

Fig. 4. Temperature distribution along the inner wall as a function of number of eigenvalues considered in the internal flow solution.

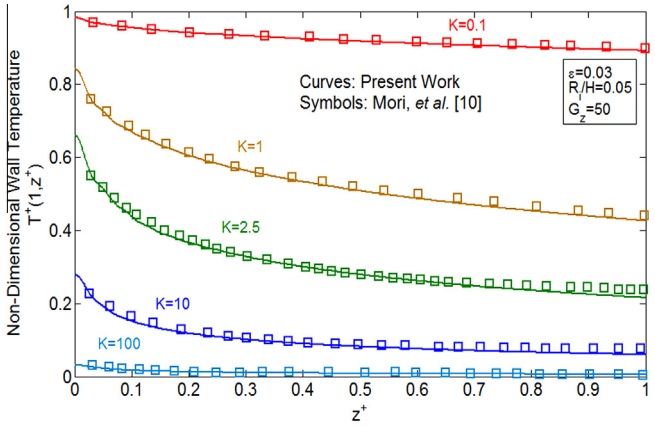

Fig. 5. Comparison of inner wall temperature as a function of axial coordinate for an internal flow problem computed using the present approach (curves) with results from Mori et al. [10] (symbols) for different ratios of solid and fluid thermal conductivities.

$$C_n^+ = \frac{-Bi_H \int_0^1 p^+(x^+)\cdot\left[\mu_n L Cos(\mu_n L x^+) + Bi_L Sin(\mu_n L x^+)\right]dx^+}{\frac{1}{2}\cdot\left[(\mu_n^2 LH + Bi_H Bi_L)\left(1+\frac{Bi_L}{(\mu_n L)^2+Bi_L^2}\right)+Bi_H\right]\cdot\left[\mu_n L Sinh(\mu_n H)+Bi_L Cosh(\mu_n H)\right]} \tag{54}$$

$$D_n^+ = \frac{\int_0^1 q_{wall}^+(x^+)\cdot\left[\mu_n L Cos(\mu_n L x^+) + Bi_L Sin(\mu_n L x^+)\right]dx^+}{\frac{1}{2}\cdot(\mu_n L)\left[(\mu_n^2 LH + Bi_H Bi_L)\left(1+\frac{Bi_L}{(\mu_n L)^2+Bi_L^2}\right)+Bi_H\right]} \tag{55}$$

$$\beta_n = \frac{(\mu_n L)Cosh(\mu_n H) - Bi_L\cdot Sinh(\mu_n H)}{(\mu_n L)Sinh(\mu_n H) + Bi_L\cdot Cosh(\mu_n H)} \tag{56}$$

The eigenvalues μ_n are obtained from roots of the transcendental equation

$$Tan(\mu L) = \frac{2Bi_L\cdot(\mu L)}{(\mu L)^2 - Bi_L^2} \tag{57}$$

where $Bi_H = \frac{hH}{k}$ and $Bi_L = \frac{hL}{k}$.

This completes the solution methodology for the external flow problem. The wall temperature determined from the solid temperature distribution may be used to repeat the process outlined above, starting with solving the fluid flow problem, which will iteratively lead to a converged solution.

Characteristics of the general methodology outlined above are discussed in the next section. Comparison with finite-element simulation results is also shown. Applications of the method for internal and external flow problems are also discussed.

3. Results and discussion

The solution methodology described and illustrated for internal and external flows in Section 2 is iterative in nature, beginning with a guessed temperature distribution along the solid–fluid interface. To understand the nature of convergence of this iterative process, two problems – one of internal flow, and another of external flow – are solved using the iterative technique. For the internal flow problem, hydrodynamically developed flow of air entering at a uniform temperature and fluid velocity of 0.5 m/s through a 0.065 m long annular cylinder with annulus diameter of 0.0026 m is considered. For the external flow problem, flow over a 0.03 m thick plate at fluid velocity of 0.01 m/s is considered. Internal heat generation of 6 W and 30 W is considered within the solid domain for the internal and external flow cases respectively. Heat transfer coefficient of 100 W/m^2 K and 50 W/m^2 K is considered along all other surfaces for the internal and external flow cases respectively. Axial and radial thermal conductivity values of 30.0 and 0.2 W/m K are assumed for the solid in the internal flow case. This models thermal conduction in systems like Li-ion cells, where thermal conduction is known to be highly orthotropic [38]. For external flow problem, an isotropic slab with thermal conductivity of 0.2 W/m K is considered. Fig. 3(a) and (b) plot the temperature distributions at the start of successive iterations along the solid–liquid interface for the internal flow and external flow problems The initial assumed wall temperature is also shown. Fig. 3(a) and (b) show excellent convergence of the temperature distribution within 4–5 iterations, even when the temperature distribution assumed initially is not accurate. An iterative

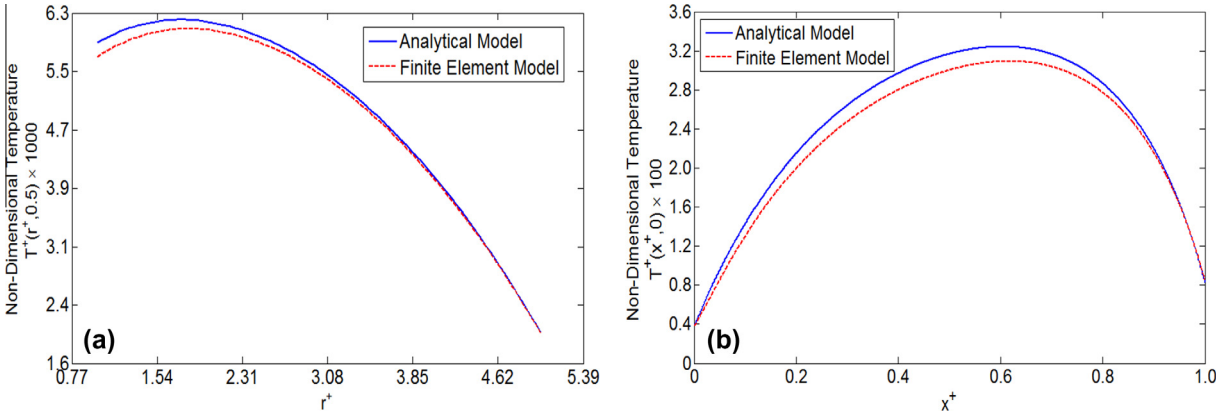

Fig. 6. (a) Comparison of temperature plot inside the solid computed using the iterative model for internal flow problem with finite element simulation results, (b) comparison of wall heat flow computed using the iterative model for external flow problem with finite element simulation results.

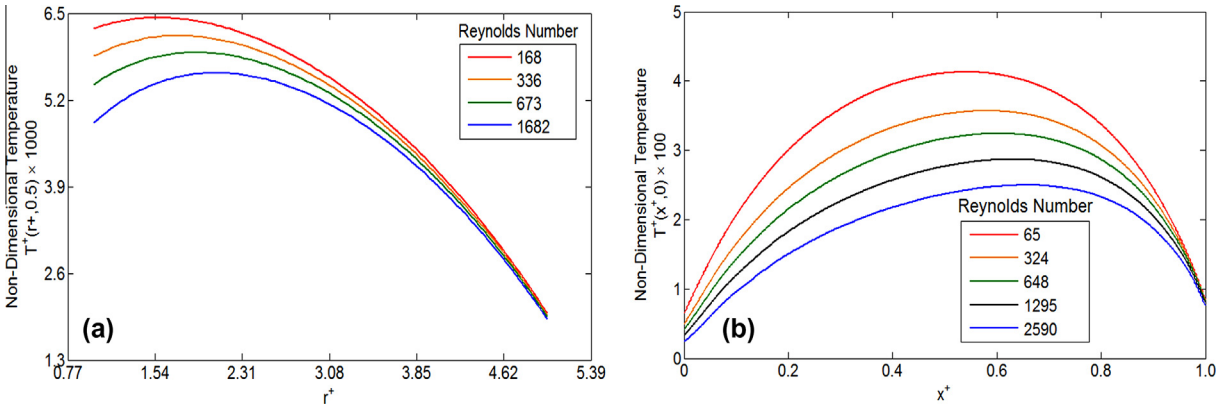

Fig. 7. (a) Solid temperature as a function of radius at mid-height for different air speeds in the internal flow problem, (b) wall temperature distribution in the external flow problem for different air speeds.

convergence criterion of change of less than 0.0002 in the non-dimensional temperature throughout the domain between successive iterations is used. In case of the internal flow problem, the accuracy of the temperature solution further depends on the number of eigenvalues considered for the infinite series solution. Fig. 4 plots the temperature distribution at the solid–liquid interface for the internal flow problem as a function of the number of eigenvalues considered. It is found that using around 8–10 eigenvalues is sufficient, and the solution does not change significantly by considering additional eigenvalues.

The analytical, iterative approach described in Section 2 is compared against results presented by Mori et al. [10] for a conjugate problem involving flow in a thick tube with constant temperature along the outside wall. Mori et al. solved this problem by assuming a power law distribution for the inner wall temperature. Fig. 5 presents the wall temperature computed from the iterative model presented here, along with results from Mori et al. [10] for five different ratios of the solid and fluid thermal conductivities. In each case, there is excellent agreement between the two temperature solutions. Further, the iterative approach presented here is compared with results from finite-element simulations, carried out in ANSYS-CFX. The parameters for problems considered for this purpose are identical to the problems in Fig. 3(a) and (b), except for a fluid speed of 0.1 m/s for the external flow. Sufficient grid refinement is carried out to ensure grid independence of results. Fig. 6(a) plots the temperature rise at mid height along the radius for the internal flow problem, using the iterative analytical model, as well as finite-element simulations. There is excellent agreement between the two. Similarly, Fig. 6(b) shows good agreement for wall heat flux for the external flow problem between the analytical model and finite-element simulation results.

Fig. 7(a) and (b) plot the temperature distributions in the solid body for internal and external flow cases respectively for a number of inlet fluid velocities. As expected, in each case, the iterative model discussed in Section 2 predicts a strong reduction in peak temperature as the fluid velocity increases. The effect of fluid velocity on the solid temperature distribution is most prominent at the wall, particularly for the internal flow case. While the wall

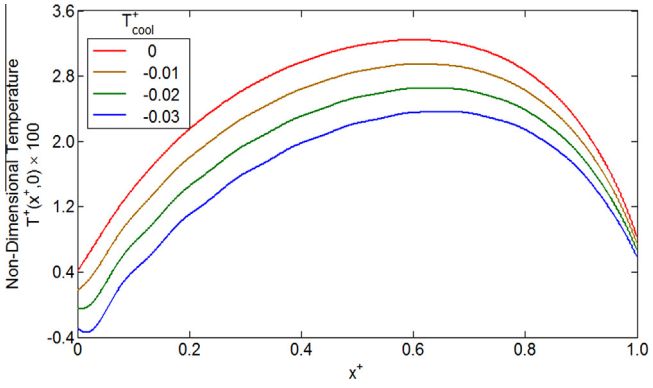

Fig. 8. Wall temperature distribution in the external flow problem for different precooling temperatures at 0.1 m/s coolant speed.

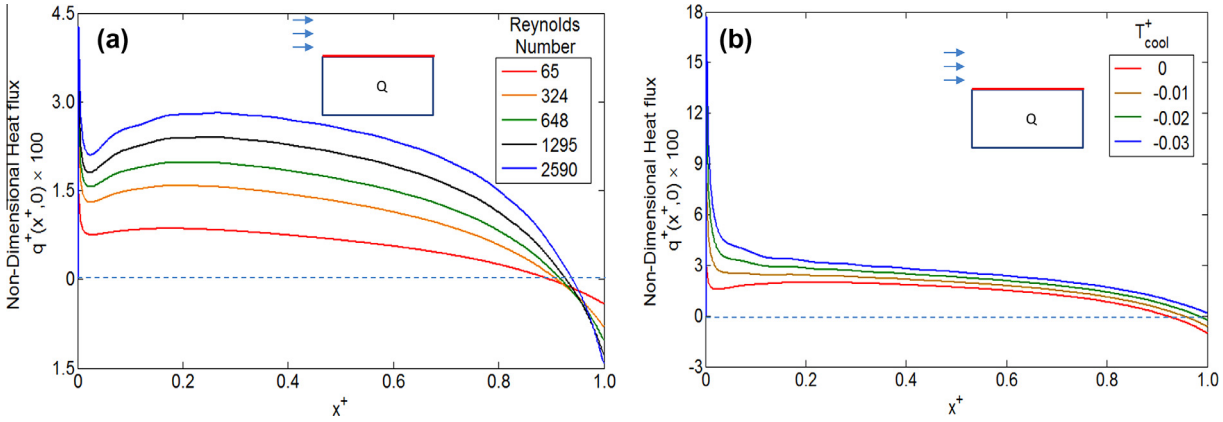

Fig. 9. (a) Wall heat flux distribution in the external flow problem for different air speeds for no precooling, (b) wall heat flux distribution in the external flow problem for different precooling temperatures at 0.1 m/s coolant speed.

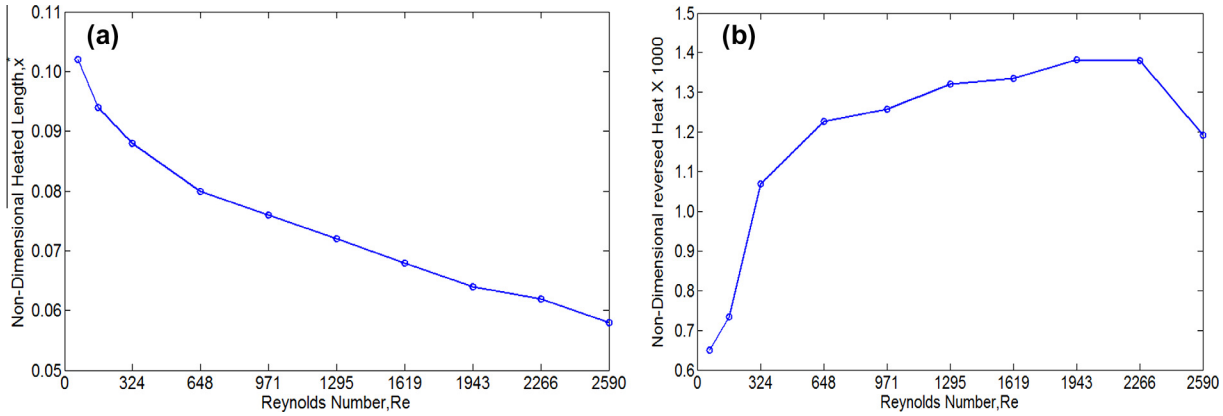

Fig. 10. Variation of the heated length in external flow as a function of air speed, (b) variation of total reversed heat in external flow problem as a function of air speed.

temperature continues to reduce as the fluid velocity is increased, this effect saturates in regions closer to the outer wall, where the effect of the coolant flow is not so prominent.

Fig. 8 presents results for the effect of precooling the inlet fluid in the external flow problem for a fluid velocity of 0.1 m/s. It is found that reducing the inlet flow temperature reduces the wall temperature distribution, plotted in Fig. 8 as a function of length along the cylinder. However, the effect is not very significant. For example, even for a precooling of −15 K, the model computations predict a peak temperature drop of only 5 K at most.

Fig. 9(a) examines the wall heat flux from the heat-generating solid into the cooling fluid as a function of the coordinate along the flow, plotted for a number of fluid flow speeds. In each case, the wall heat flux is positive for nearly the entire length, except for a small region towards the end. In this region, the sign of the heat flux reverses, and heat flows back from the fluid into the solid. This interesting phenomenon occurs because as the fluid traverses the length of the solid, it progressively gets hotter, so that beyond a certain critical length, the heat flow direction reverses, and the fluid actually starts heating up the solid. This interesting behavior is seen at all fluid speeds. In Fig. 9(b), the wall heat flux is plotted along the length of the plate at fluid velocity of 0.1 m/s at different precool temperatures. It is evident that precooling reduces the length over which reversal of heat flow occurs. Precooling may not affect the peak temperature of the plate significantly but may reduce or eliminate the local heating of the plate near the end region. Such reversal in the direction of heat flow has been reported in the past for heat transfer from a sphere in the wake region [39].

As shown in Fig. 10(a), the location of heat flux reversal moves further downstream as the fluid velocity increases. On the other hand, the magnitude of the reversed heat flux also increases with increase in fluid velocity. Therefore, Fig. 10(a) alone is not sufficient in knowing whether the overall reversed heat decreases with increase in fluid velocity. In Fig. 10(b), total reversed heat flow is plotted against fluid velocity by integrating the reversed heat flux over the heated length. The total reversed heat increases with increase in velocity up to a certain velocity, after which it starts going down. These plots may be useful in deciding the appropriate fluid velocity, and whether precooling may be helpful in the case of cooling a heat-generating solid with external flow.

4. Conclusions

The iterative analytical methodology presented in this paper is a general method for solving conjugate heat transfer problems involving both conduction and convection. This approach is simpler and mathematically less involved compared to other approaches reported earlier. Results based on this approach are in good agreement with a past method and with finite-element simulations. While this method is illustrated in this paper for two specific example problems involving internal and external flows, other more complicated scenarios, for example, involving multiple solid–fluid interfaces, can also be analyzed. The iterative

approach presented here may help improve the fundamental understanding of conjugate heat transfer, as well as develop thermal modeling tools for applications where conjugate heat transfer is important.

Conflict of interest

None declared.

References

[1] W.M. Kays, M.E. Crawford, Convective Heat and Mass Transfer, McGraw-Hill, New York, 1993.
[2] R.K. Shah, A.L. London, Laminar flow forced convection in ducts, in: Advances in Heat Transfer, Academic Press, New York, 1978.
[3] L. Graetz, Über die warmeleitungsfahigheit von flussingkeiten, part 1, Ann. Phys. Chem. (1883).
[4] M. Jacob, Heat Transfer, first ed., John Wiley & Sons, New York, 1949.
[5] E.R.G. Eckert, R.M. Drake, Heat and Mass Transfer, McGraw-Hill, 1959.
[6] E.M. Sparrow, H.S. Yu, Local non-similarity thermal boundary-layer solutions, J. Heat Transfer 93 (1971) 328–334.
[7] J.R. Sellars, M. Tribus, J.S. Klein, Heat transfer to laminar flow in a round tube or flat conduit — the Graetz problem extended, Trans. ASME 78 (1956) 441–448.
[8] M. Tribus, J.S. Klein, Forced convection from nonisothermal surfaces, in: Proc. Heat Transfer Symp., University of Michigan Engineering Research Institute, 1953, pp. 211–235.
[9] X. Yin, H.H. Bau, The conjugate Graetz problem with axial conduction, J. Heat Transfer 118 (1996) 482–485.
[10] S. Mori, M. Sakakibara, A. Tanimoto, Steady heat transfer to laminar flow in a circular tube with conduction in the tube wall, Heat Transfer Jpn. Res. 3 (1974) 37–46.
[11] A.V. Luikov, V.A. Aleksashenko, A.A. Aleksashenko, Analytical methods of solution of conjugated problems in convective heat transfer, Int. J. Heat Mass Transfer 14 (1971) 1047–1056.
[12] J. Gosse, Analyse simplifiée du couplage conduction-convection pour un écoulement à couche limite laminaire sur une plaque plane, Rev. Gen. Therm. 228 (1980) 967–971.
[13] T.L. Perelman, On conjugated problems of heat transfer, Int. J. Heat Mass Transfer 3 (1961) 293–303.
[14] M. Faghri, E.M. Sparrow, Simultaneous wall and fluid axial conduction in laminar pipe-flow heat transfer, J. Heat Transfer 102 (1980) 58–63.
[15] R.K. Shah, M.S. Bhatti, Laminar convective heat transfer in ducts, in: S. Kakac, R.K. Shah, W. Aung (Eds.), Handbook of Single-phase Convective Heat Transfer, John Wiley, New York, 1987.
[16] K. Shah, A. Jain, Modeling of steady-state and transient thermal performance of a Li-ion cell with an axial fluidic channel for cooling, Int. J. Energy Res. 39 (2015) 573–584.
[17] M.N. Ozisik, Heat Conduction, second ed., John Wiley & Sons, 1993.
[18] H.S. Carslaw, J.C. Jaegar, Conduction of Heat in Solids, second ed., Clarendon Press, 1959.
[19] A.S. Dorfman, Conjugate Problems in Convective Heat Transfer, CRC Press, 2009.
[20] B. Weigand, G. Gassner, The effect of wall conduction for the extended Graetz problem for laminar and turbulent channel flows, Int. J. Heat Mass Transfer 50 (2007) 1097–1105.
[21] V.A. Aleksashenkto, The steady conjugated problem of heat transfer in fluid flow in a semi-infinite tube including the effect of viscous dissipation, J. Eng. Phys. 14 (1968) 100–108.
[22] S. Mori, T. Shinke, M. Sakakibara, A. Tanimoto, Steady heat transfer to laminar flow between parallel plates with conduction in the wall, Heat Transfer Jpn. Res. 3 (1974) 37–46.
[23] C.A. Deavours, An exact solution for the temperature distribution in parallel plate Poiseuille flow, J. Heat Transfer 96 (1974) 489–495.
[24] R.O.C. Guedes, M.N. Ozisik, Conjugated turbulent heat transfer with axial conduction in wall and convection boundary conditions in a parallel-plate channel, Int. J. Heat Mass Transfer 13 (1992) 322–328.
[25] A. Lehtinen, R. Karvinen, Analytical solution for a class of flat plate conjugate convective heat transfer problems, Front. Heat Mass Transfer 2 (2011) 043004.
[26] G.S. Barozzi, G. Pagliarini, A method to solve conjugate heat transfer problems: the case of fully developed laminar flow in a pipe, J. Heat Transfer 107 (1985) 77–83.
[27] A. Pozzi, M. Lupo, Coupling of conduction with forced convection over a flat plate, Int. J. Heat Mass Transfer 32 (1989) 1207–1214.
[28] S. Bilir, Laminar flow heat transfer in pipes including two-dimensional wall and fluid axial conduction, Int. J. Heat Mass Transfer 38 (1995) 1619–1625.
[29] P.I. Jagad, B.P. Puranik, A.W. Date, An iterative procedure for the evaluation of a conjugate condition in heat transfer problems, Numer. Heat Transfer Part A Appl. 61 (2012) 353–380.
[30] R. Karvinen, Some new results for conjugate heat transfer in a flat plate, Int. J. Heat Mass Transfer 21 (1978) 1261–1264.
[31] A. Campo, C. Schuler, Heat transfer in laminar flow through circular tubes accounting for two-dimensional wall conduction, Int. J. Heat Mass Transfer 31 (1988) 2251–2259.
[32] I. Pop, D.B. Ingham, A note on conjugate forced convection boundary-layer flow past a flat plate, Int. J. Heat Mass Transfer 36 (1993) 3873–3876.
[33] M. Vynnycky, S. Kimura, K. Kanev, I. Pop, Forced convection heat transfer from a flat plate: the conjugate problem, Int. J. Heat Mass Transfer 41 (1998) 45–59.
[34] L. Choobineh, A. Jain, Determination of temperature distribution in three-dimensional integrated circuits (3D ICs) with unequally-sized die, Appl. Therm. Eng. 56 (2013) 176–184.
[35] L. Choobineh, A. Jain, Analytical solution for steady-state and transient temperature field in vertically integrated three-dimensional integrated circuits (3D ICs), IEEE Trans. Compon. Packag. Manuf. Technol. 2 (2012) 2031–2039.
[36] A. Haji-Sheikh, J.V. Beck, D. Agonafer, Steady-state heat conduction in multilayer bodies, Int. J. Heat Mass Transfer 46 (2003) 2363–2379.
[37] S.J. Drake, M. Martin, D.A. Wetz, J.K. Ostanek, S.P. Miller, J.M. Heinzel, A. Jain, Heat generation rate measurement in a Li-ion cell at large C-rates through temperature and heat flux measurements, J. Power Sources 285 (2015) 266–273.
[38] S.J. Drake, D.A. Wetz, J.K. Ostanek, S.P. Miller, J.M. Heinzel, A. Jain, Measurement of anisotropic thermophysical properties of cylindrical Li-ion cells, J. Power Sources 252 (2014) 298–304.
[39] B. Abramzon, C. Elata, Unsteady heat transfer from a single sphere in stokes flow, Int. J. Heat Mass Transfer 27 (1984) 687–695.